

AD-A184 351

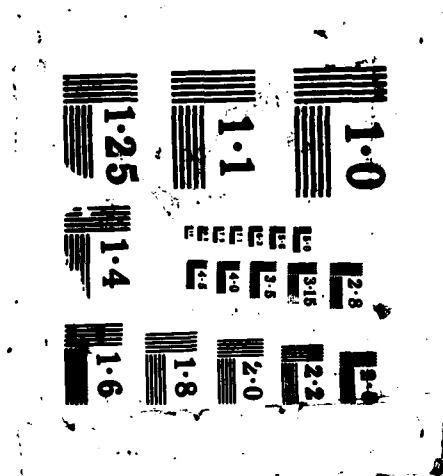
APPLICATION OF LATTICE FILTERING TECHNIQUES TO CW  
MEASURED TIME DOMAIN DATA(U) LAWRENCE LIVERMORE  
NATIONAL LAB CA 5 GILES ET AL JAN 87 N00014-83-D-0689  
F/G 9/1

1/1

UNCLASSIFIED

NL





DTIC FILE COPY

(12)

AD-A184 351

APPLICATION OF LATTICE FILTERING TECHNIQUES  
TO CW MEASURED TIME DOMAIN DATA

S. Giles  
H. G. Hudson  
S. R. Parker  
R. J. King

N00014-83-D-0689

January 1987

DTIC  
ELECTE  
SEP 02 1987  
S D  
CLD

DISTRIBUTION STATEMENT A  
Approved for public release;  
Distribution Unlimited

This work was supported by the Office of Naval Technology/American Society of Engineering Education. The work was performed at the Lawrence Livermore National Labs.

87 9 1 057

## INTRODUCTION

This paper concerns the application of lattice filtering [1,2,3] techniques to discrete frequency domain data. Time domain models for two different antennas are found, the monopole and cavity-back spiral. Lattice models and a layered medium model [4,5] are obtained.

The following is a brief list of important notation used in the work, basically that of Parker [1].

$N$	Number time domain sampled points
$y_i$	Discrete time domain signal
$e_{mn}$	Forward prediction error
$\bar{e}_{mn}$	Backward prediction error
$T_s$	Time domain sampling period
$Y_l$	Discrete Fourier transform of $y_i$
$R_i$	Autocorrelation coefficient of lag $i T_s$
$k_i$	Reflection (partial correlation) coefficient
$\omega_0$	Fundamental angular frequency
$m$	Order of difference equation for $y_i$ s
$b_{ml}$	$l$ th coefficient in difference equation for $y_i$ s
$W_R$	Right going planar wave
$W_L$	Left going planar wave
$u_l$	Wave propagation speed in boundary $l$
$\eta_l$	Characteristic impedance in boundary $l$
$z^{-1}$	Single sampling period delay



per call	
Distribution/	
Availability Codes	
Dist	Avail and/or Special
A-1	

## PRODUCTION OF AUTOCORRELATION COEFFICIENTS

We assume all  $Y_i(l\omega_0)$   $i=0, \dots, m$  are known. The method by which these complex quantities are obtained is immaterial. However, for this work they were obtained through experiments using the EMP Engineering Research Omnidirectional Radiator (EMPEROR), the heart of which is an HP8510 Network Analyzer.

The calculation of  $R_i$   $i=0, \dots, m$  is straight forward.

$$R_i = |Y_0|^2 + \frac{1}{2} \sum_{l=1}^m |Y_l|^2 \cos l \omega_0 i T_s \quad i=0, \dots, m. \quad (1)$$

$\omega_0$  is related to the sampling period in equation (1) by

$$\omega_0 = \frac{2\pi}{[2m+1]_{2p} T_s} \quad (2)$$

where  $[2m+1]_{2p}$  is the nearest power 2 operator on  $2m+1$ . The number ( $N$ ) of time samples is taken to be  $[2m+1]_{2p}$ .  $R_i$  is useful in determining an estimate of  $y_i$   $i=0, \dots, N-1$ .

## PRODUCTION OF LATTICE STRUCTURES

For a linear causal stationary real autoregressive (AR) process of order  $m$ , the forward prediction error is given by

$$e_{mn} = y_n - \sum_{l=1}^m b_{ml} y_{n-l} \quad n = 0, \dots, N-1. \quad (3)$$

The backward prediction error (sometimes called postdiction error) is the following expression:

$$\bar{e}_{mn} = y_{n-m} - \sum_{l=1}^m b_{ml} y_{n-m+l} \quad n = 0, \dots, N-1. \quad (4)$$

The  $b_{ml}$ s in equations (3) and (4) are the difference equation coefficient for an AR process of order  $m$ . It is assumed that  $e_{mn}$  and  $\bar{e}_{mn}$  have the same statistical properties, that  $\bar{e}_{0n} = e_{0n} = y_n$ , and that  $m \leq 250$ .

Using the Levinson-Durbin algorithm and equations (3) and (4) we can write the following important relations:

$$e_{m+1,n} = e_{mn} - k_{m+1} \bar{e}_{m,n-1} \quad (5)$$

$$\bar{e}_{m+1,n} = -k_{m+1} e_{mn} + \bar{e}_{m,n-1} \quad (6)$$

where the quantity  $k_{m+1}$  (reflection coefficient) is given by either the expectation

$$k_{m+1} = \frac{E(e_{mn} \bar{e}_{m,n-1})}{E(|\bar{e}_{m,n-1}|^2)} \quad (7)$$

ratio or equivalently

$$k_{m+1} = b_{m+1,m+1} \quad (8)$$

Another way of calculating the  $k$ -values is to use the Shur algorithm [6], since by now the  $R_i$ s are known. This algorithm involves the following steps:

1. Define a generator matrix

$$\begin{matrix} T \\ G \\ 0 \end{matrix} = \begin{bmatrix} R_0 & R_1 & \dots & R_m \\ 0 & R_1 & \dots & R_m \end{bmatrix} \quad (9)$$

2. Shift the first column of the generator matrix and define

$$\begin{matrix} T \\ \bar{G} \\ 1 \end{matrix} = \begin{bmatrix} 0 & R_0 & \dots & R_{m-1} \\ 0 & R_1 & \dots & R_m \end{bmatrix} \quad (10)$$

3. Calculate  $k_1$

$$k_1 = \frac{R_1}{R_0} \quad (11)$$

4. Define a matrix  $\theta(k_1)$

$$\theta = \frac{1}{\sqrt{1-k_1^2}} \begin{bmatrix} 1 & -k \\ -k & 1 \end{bmatrix} \quad (12)$$

5. Produce new generator matrix

$$\begin{matrix} T \\ G \\ 1 \end{matrix} = \theta(k_1) \begin{matrix} T \\ \bar{G} \\ 1 \end{matrix} \quad (13)$$

6. Go to step 2 and repeat until all ks are found.

We have used the above algorithm to calculate k-values.

Equations (5) and (6) can be represented by the basic lattice diagram (Fig. 1). We shall call this

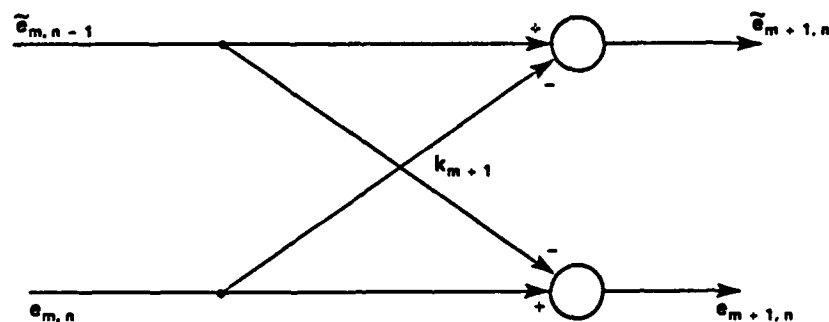


Figure 1. Basic Lattice Structure ( $k_{m+1}^2 \neq 1$ )

structure the transmission lattice as will become obviously justified from the following lattice, which we shall call the scattering lattice (Fig. 2). From the scattering lattice it is clear that the backward error and forward error can be viewed as right going

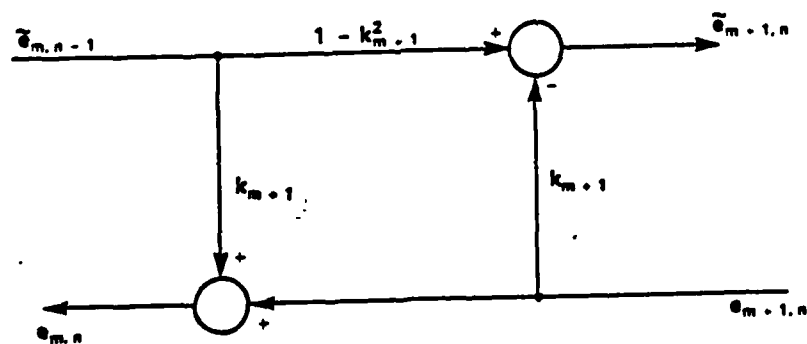


Figure 2. Scattering Lattice Structure ( $k_{m+1}$ )



and left going signals, respectively; and the transmission lattice relates quantities at one port with those at the other port.

If we drop the second subscript on the error and represent single sampling period delays by  $z^{-1}$ , the transmission lattice looks like this (Fig. 3).

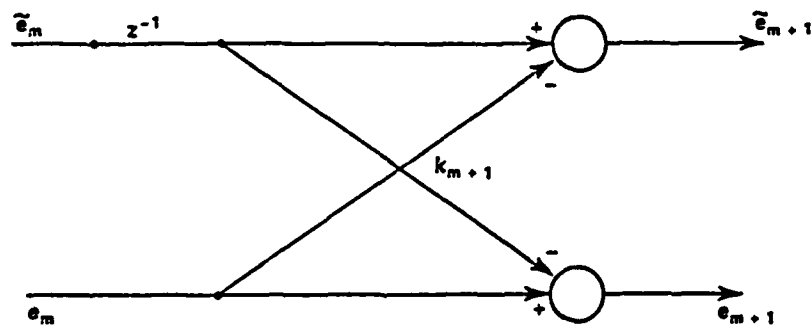


Figure 3. Transmission Lattice  $z^{-1}$  Delay

By cascading transmission lattice we can produce a "whitening" filter as shown in Fig. 4. That is,

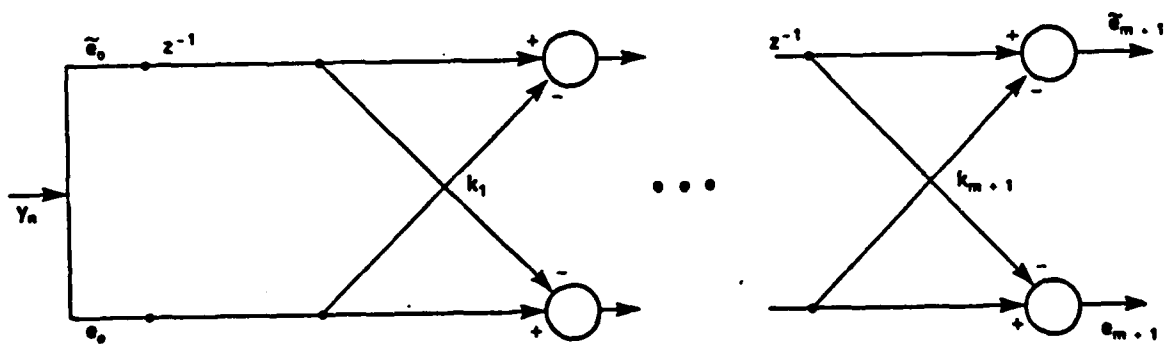


Figure 4. Whitening Filter

from Fig. 4 we have a relationship between the outputs  $\bar{e}_{m+1}$  and  $e_{m+1}$  and the single input  $y_i$  of the following form:

$$\begin{bmatrix} \bar{e}_{m+1} \\ e_{m+1} \end{bmatrix} = T \begin{bmatrix} \bar{e}_0 \\ e_0 \end{bmatrix} \quad (14)$$

where the matrix  $T$  is the overall transmission matrix:

$$T = \begin{bmatrix} 1 & -k_{m+1} \\ -k_{m+1} & 1 \end{bmatrix} \begin{bmatrix} Z^{-1} & 0 \\ 0 & 1 \end{bmatrix} \begin{bmatrix} 1 & -k_m \\ -k_m & 1 \end{bmatrix} \begin{bmatrix} Z^{-1} & 0 \\ 0 & 1 \end{bmatrix} \dots \begin{bmatrix} 1 & -k_1 \\ -k_1 & 1 \end{bmatrix} \begin{bmatrix} Z^{-1} & 0 \\ 0 & 1 \end{bmatrix} \quad (15)$$

Now, one can examine the  $T_{22}$  entry of  $T$  for the characteristic equation or use Levinson-Durbin to calculate the AR parameters. Before leaving the transmission matrix we consider the case when error signals are delayed according to a factor  $z^{-\beta}$ , where  $\beta$  is a constant. It follows from equations (5) and (6) that the lattice structure will be as shown in Fig. 5.

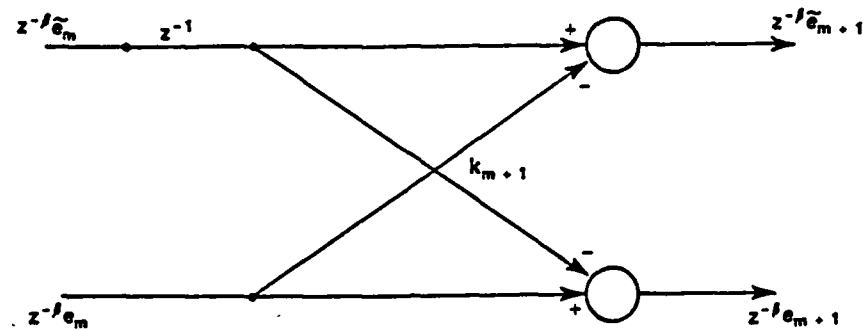


Figure 5. Transmission Lattice Delay  $Z^{-\beta}$  in Each Branch

Cascading scattering lattices without the  $z^{-\beta}$  factor, we generate the following filter (Fig. 6), which was used to predict  $y_n$   $n=0,1,\dots,N-1$ . By driving the filter at the  $e_{m+1}$  terminal with a shifted pulse, we

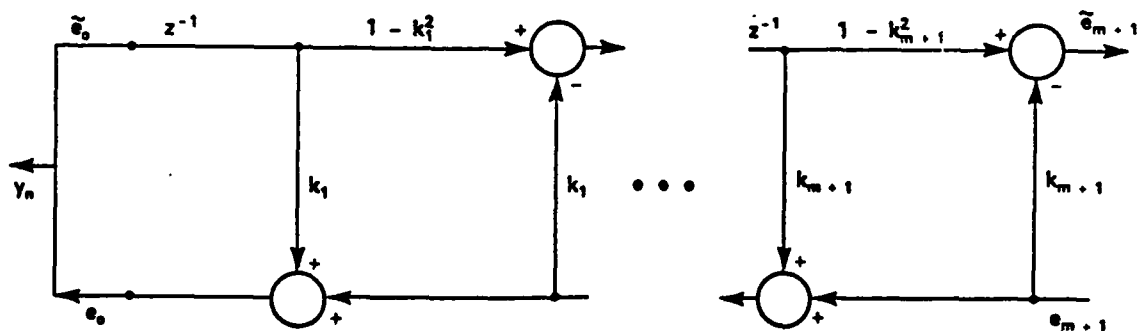


Figure 6. Cascaded Scattering Lattices

obtain a response which estimates the original discrete time signal,  $y_i$ . If we include the  $z^{-\beta}$  factors in each basic lattice, we get the diagram shown in Fig. 6 but with  $z^{-\beta}$  delays with the  $\tilde{e}_0$  and  $e_0$  signals treated appropriately. The  $z^{-\beta}$  factor is important in considerations of EM waves in layered media.

## WAVES IN A LAYERED MEDIUM

We assume from an EM field theory point of view that the source free medium of interest is linear and stationary, but that it is divided into sections which are anisotropic and homogeneous bounded by short sections of materials which are isotropic and nonhomogeneous. We assume that right going and left going planar waves exist in the different media which make up the overall medium and variations in  $y$  and  $z$  directions are negligible. Figure 7 depicts this situation [5].

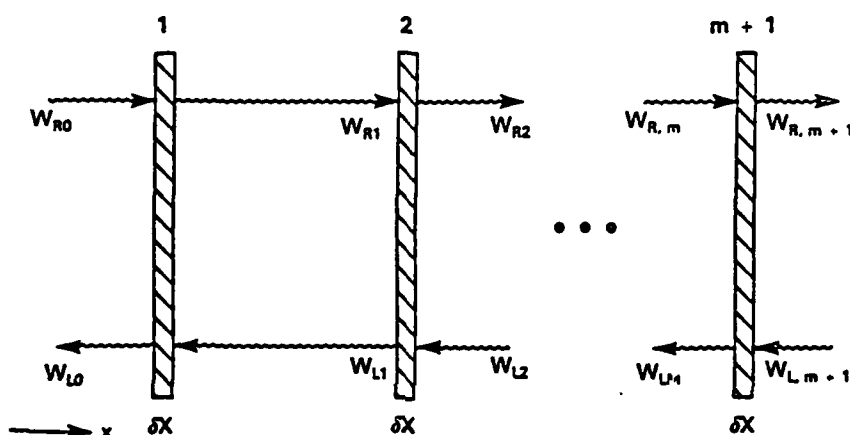


Figure 7. Layered Medium.

The sections numbered 1 to  $m+1$  and shaded are the isotropic -- but not necessarily homogeneous -- boundaries. Between the boundaries are sections of anisotropic homogeneous materials. To the right of boundary  $m+1$  and left of 1 are infinite isotropic homogeneous regions.

Considering the boundaries first, from transmission line theory, we can write after a few manipulations the relationship between right and left going waves as the following [4]:

$$\frac{\partial}{\partial x} \begin{bmatrix} W_R \\ W_L \end{bmatrix} = \begin{bmatrix} -\frac{1}{u_l} \frac{\partial}{\partial t} & -\alpha_l(x) \\ -\alpha_l(x) & \frac{1}{u_l} \frac{\partial}{\partial t} \end{bmatrix} \begin{bmatrix} W_R \\ W_L \end{bmatrix} \quad (16)$$

For the  $l$ th section  $\alpha_l(x)$  in operator equation (16) is given by

$$\alpha_l(x) = \frac{1}{2\eta_l} \frac{\partial \eta_l}{\partial x} \quad (17)$$

where  $\eta_l$  is a function of position. We can solve equation (17) for  $\eta_l$ , i.e.,

$$\eta_l(x) = A \exp \left[ 2 \int^x \alpha_l(\lambda) d\lambda \right] \quad (18)$$

where  $A$  is a constant. Now, it can be shown using forward discretization with step sizes  $\Delta x$  and  $\Delta t$  and for small  $\frac{1}{u_l} \frac{\Delta x}{\Delta t}$  factors that the scattering lattice structure for equation (16) is the following:

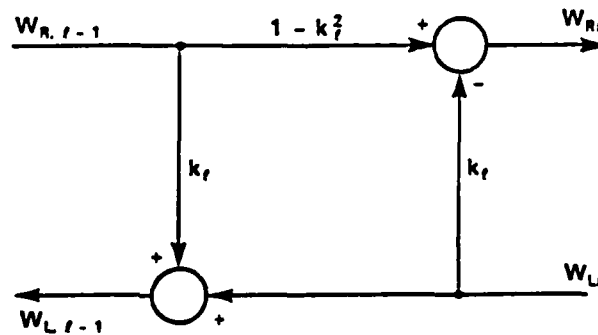


Figure 8. Transmission line lattice for boundary  $l$  ( $l = 1, \dots, m+1$ )

$k_l$  in the above Fig. 8 is  $\bar{\alpha}_l \delta x$ , where  $\bar{\alpha}_l$  is the average value of  $\alpha_l$  in the boundary  $l$ . For a very small magnitude value  $k_l$  is approximately the reflection coefficient of EM wave theory. From Fig. 8 we recognize that  $W_{R, m+1}$  is analogous to  $\bar{e}_{m+1}$  and that  $W_{L, m+1}$  is like  $e_{m+1}$ . The only problem is the representation of the delay in the basic scattering lattice of Fig. 2.

This problem can be rectified by considering waves in regions between boundaries. We simply use the propagation times to establish the delays. Since the medium is homogenous between boundaries, corresponding reflection coefficients are zeros and the scattering lattices are sections of straight lines. Then it follows that the  $z^{-\beta}$  factor ( $\beta \neq 0$ ) of Fig. 5 represents the time it takes a left going wave to be emitted by one boundary and propagate to the next boundary. Since from the basic lattice structure analogous right going "waves" must take longer than left going ones (the  $z^{-1}$  factor), the material between boundaries must be anisotropic with propagation speed in one direction different from that in the opposite direction. So, not only do we have the lattice models of Figs. 4 and 6, we also have a layered medium model which will have the structure of Fig. 9.

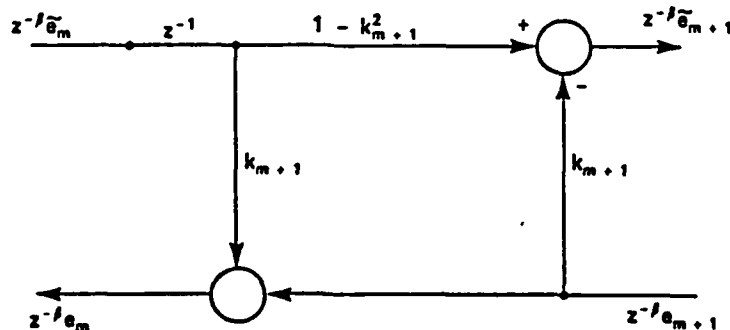


Figure 9. Basic Layered Medium Lattice for Errors

## RESULTS

The above modeling theory was applied to data obtained for experimental use of EMPEROR where a 22.5 cm monopole was used as a test object. The response of the monopole for 250 k-values and for 15 non-zero k-values modeling was obtained. The reduced order (15 non-zero k-values) cases result from setting statistically insignificant k-values equal to zeros, and correspond to elimination of certain exponentially damped sinusoidal components. Discrete Fourier transforms (DFT) and time estimate signals are shown in Figs. 10-18. The only problem in producing these results was selecting the proper shift for the input pulse. This was done by trying different shifts until the DFT of the estimate time signal matched that of the measured frequency domain data.

In Figs. 19-21 is shown how well the scheme performs for a more complicated antenna test object, the cavity-backed spiral antenna. These values were reproduced for 250 k-values, only. As in the monopole case the lattice model does yield agreeable results for frequency domain. For time domain, the results for CB spiral are not as good as those for the monopole.

## CONCLUSIONS

It has been shown that autocorrelation coefficients and reflection coefficients are key quantities in structuring lattice models. It has been shown that frequency domain data can be used to build time domain lattice models. It has been demonstrated that the method works for monopole and cavity-backed spiral antenna data.

#### REFERENCES

1. Parker, S. R., "Lattice Modeling of Stochastic Signals: Some Fundamental Concepts." LLNL/UCRL 15802, SIC 4343905, 1986.
2. Makhoul, John, "Linear Prediction: A Tutorial Review," Proceedings of IEEE, Vol. 63, April 1975, pp. 561-580.
3. Kay, S. M. and S. L. Marble, "Spectrum Analysis--A Modern Perspective," Proceedings of IEEE, Vol. 69, November 1981, pp. 1380-1419.
4. Bruckstein, A. M., B. C. Levy and T. Kailath, "Differential Methods in Inverse Scattering," SIAM Journal of Applied Mathematics, Vol. 45, April 1985, pp. 312-335.
5. Orfanidis, S. J., Optimum Signal Processing: An Introduction. New York: Macmillan Publishing Company, 1986.
6. Dewilde, P., A. C. Vieira and T. Kailath, "On a Generalized Szegő - Levinson Realization Algorithm for Optimal Linear Predictors Based on a Network Synthesis Approach," IEEE Transactions on Circuits and Systems, Vol. CAS-25, September 1978, pp. 663-675.



3-DEC-86 09:40:45

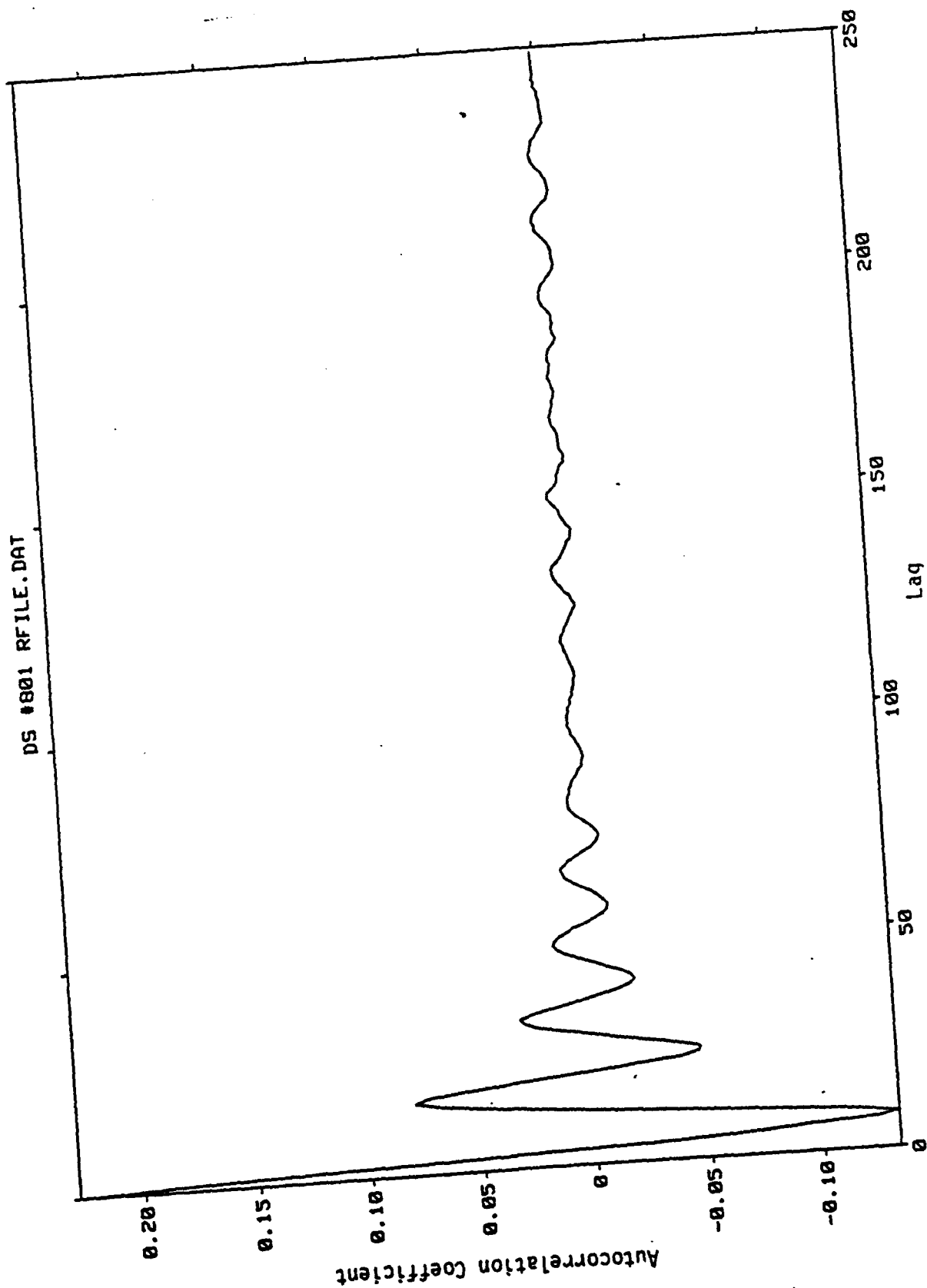


Figure 10. Autocorrelation 22.5 cm Monopole

DS #800 KFILE.DAT

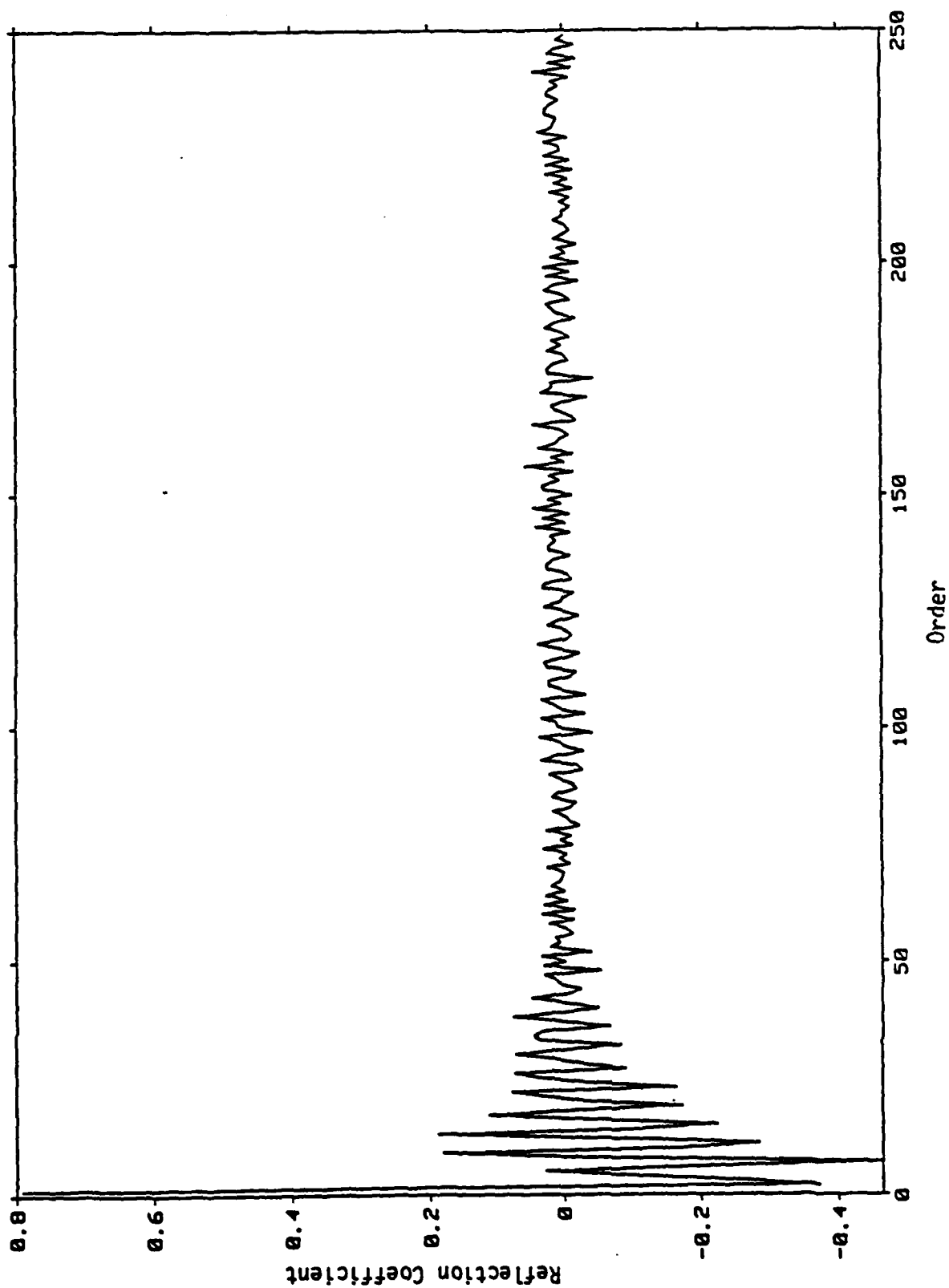


Figure 11. Reflection Coefficient 22.5 cm Monopole  
(250 nonzero k-values)

sig

DS #831 K-VALUES/EC=.08/L15

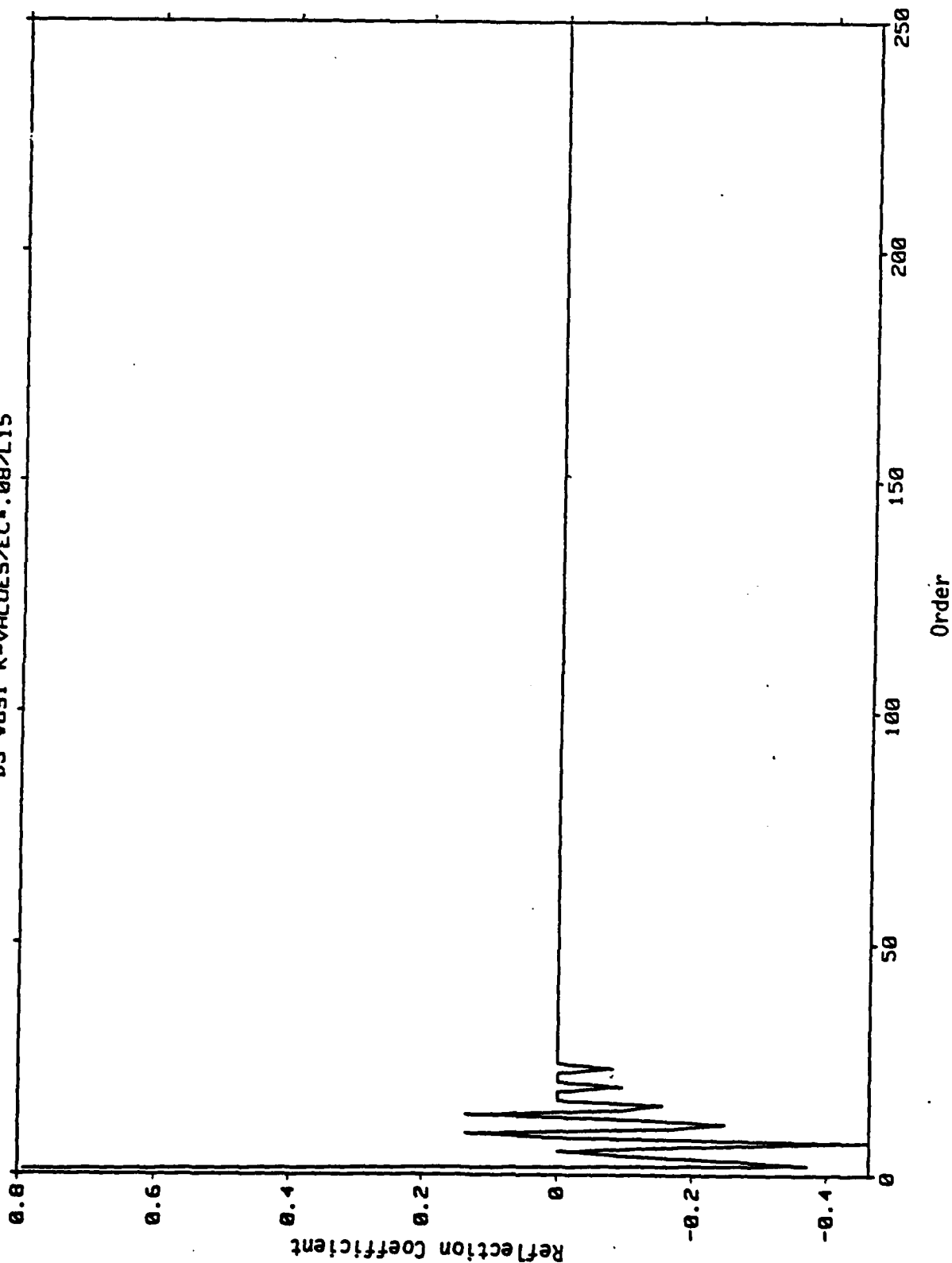


Figure 12. Reflection Coefficient 22.5 cm Monopole  
(15 nonzero k-values)

sig

9-DEC-86 11:48:06

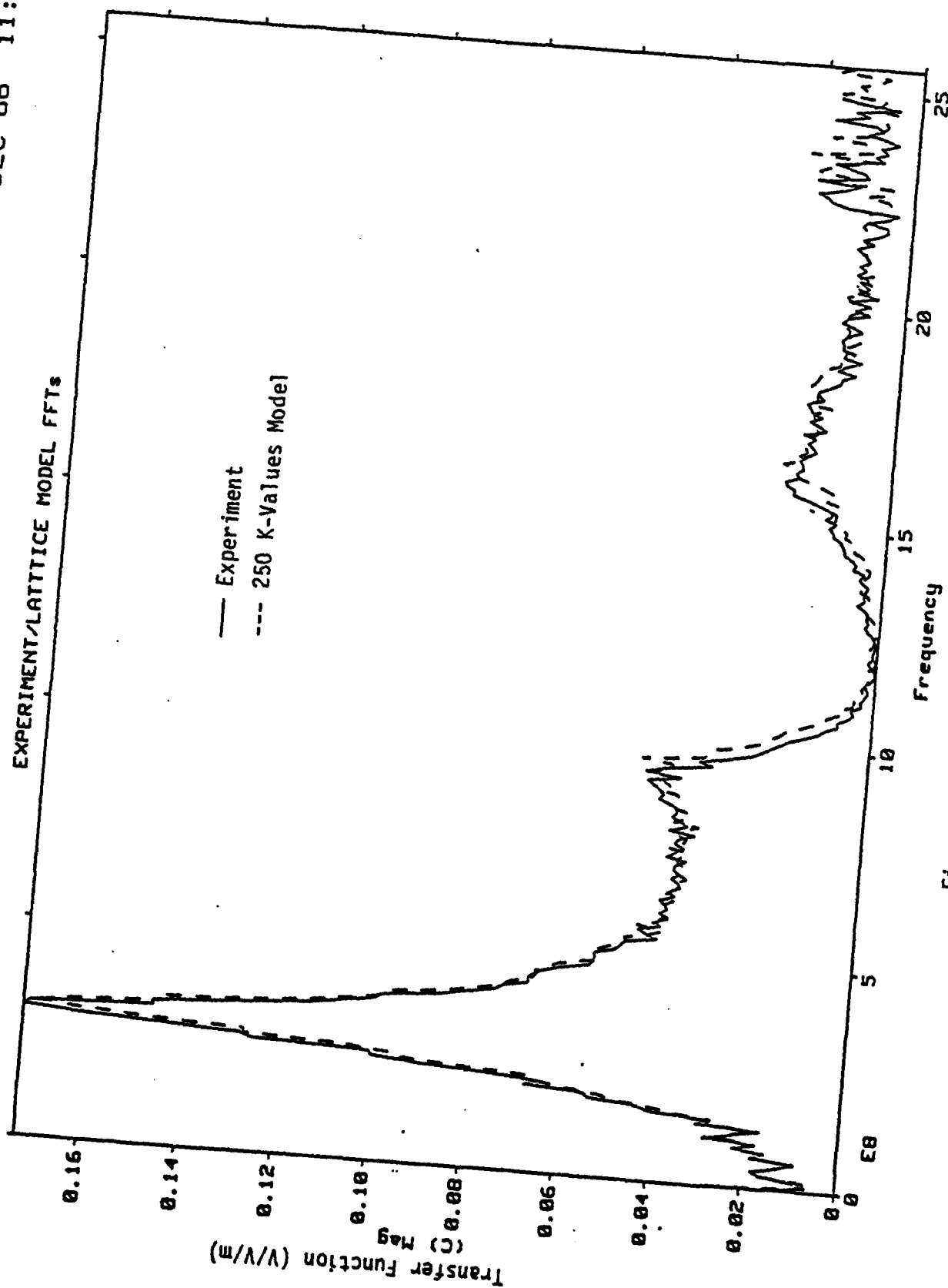


Figure 13. Monopole FFT ( 250 k-values)

sig

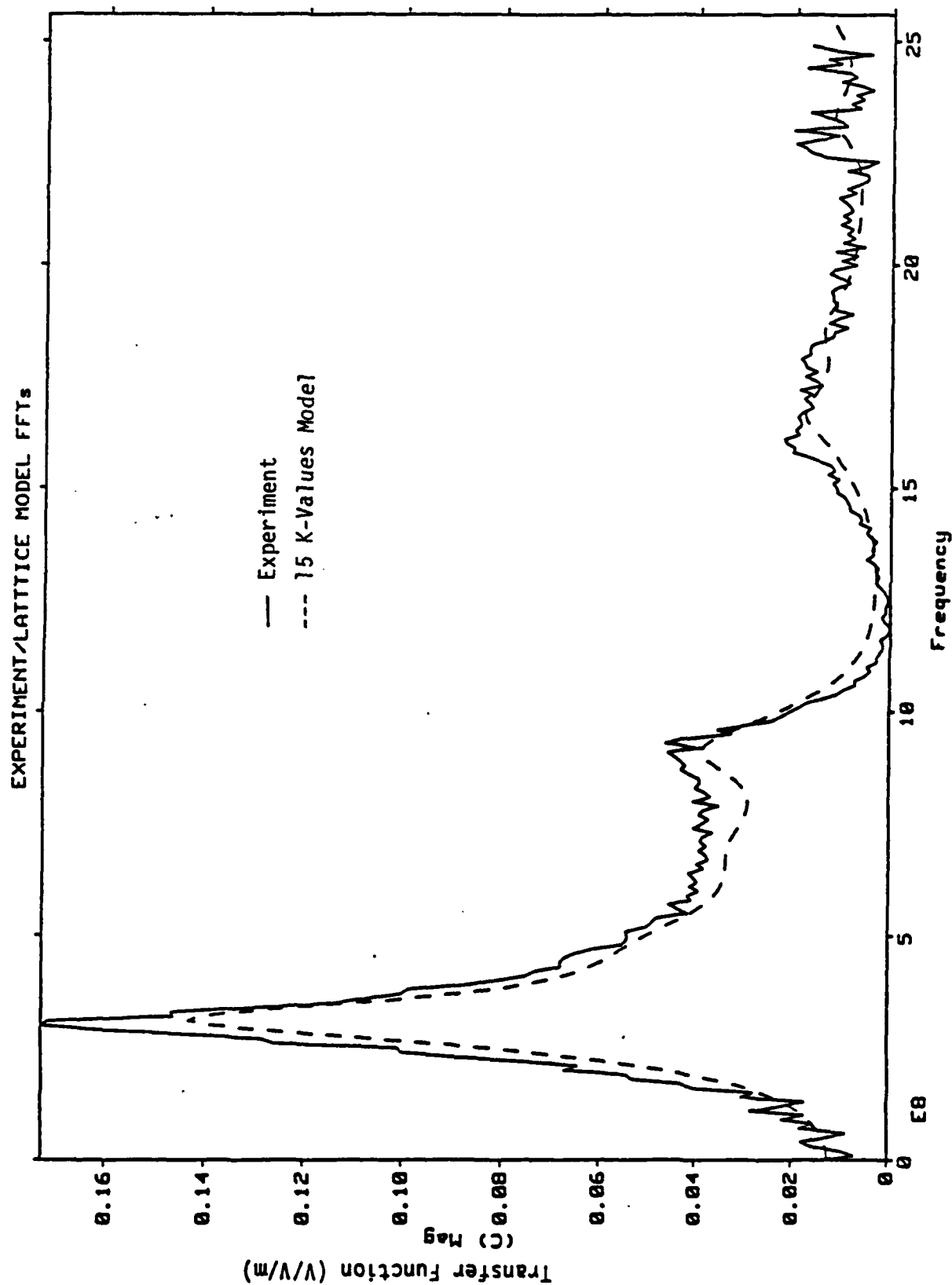


Figure 14. Monopole FFT (15 k-values)

sig

DS #850 PLOT.DAT

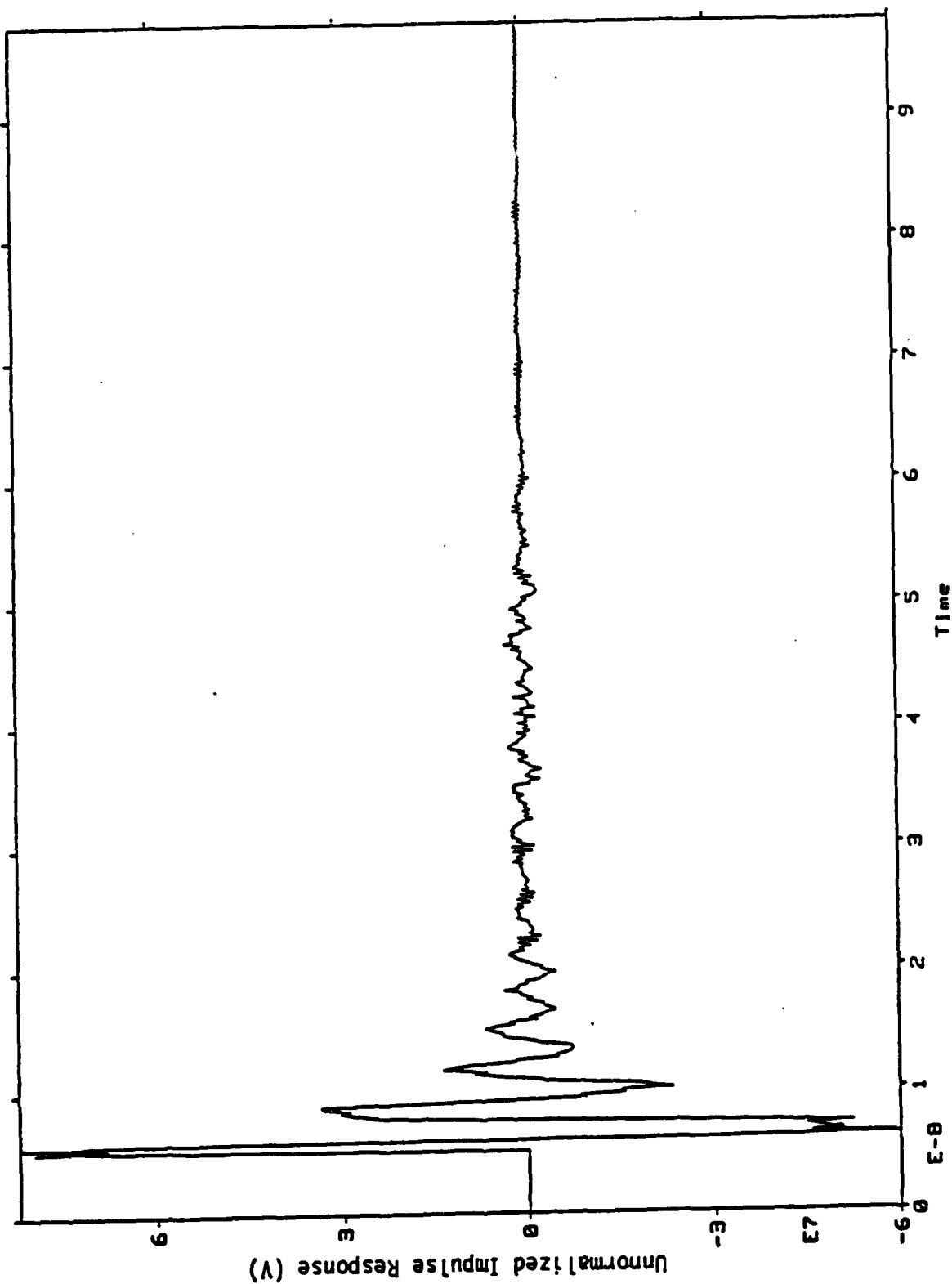


Figure 15. Simulated monopole Reponse (250 k-values)

sig

17-DEC-86 00:43:36

DS #832 22.5 MONOPOLE/EC-.008/L15

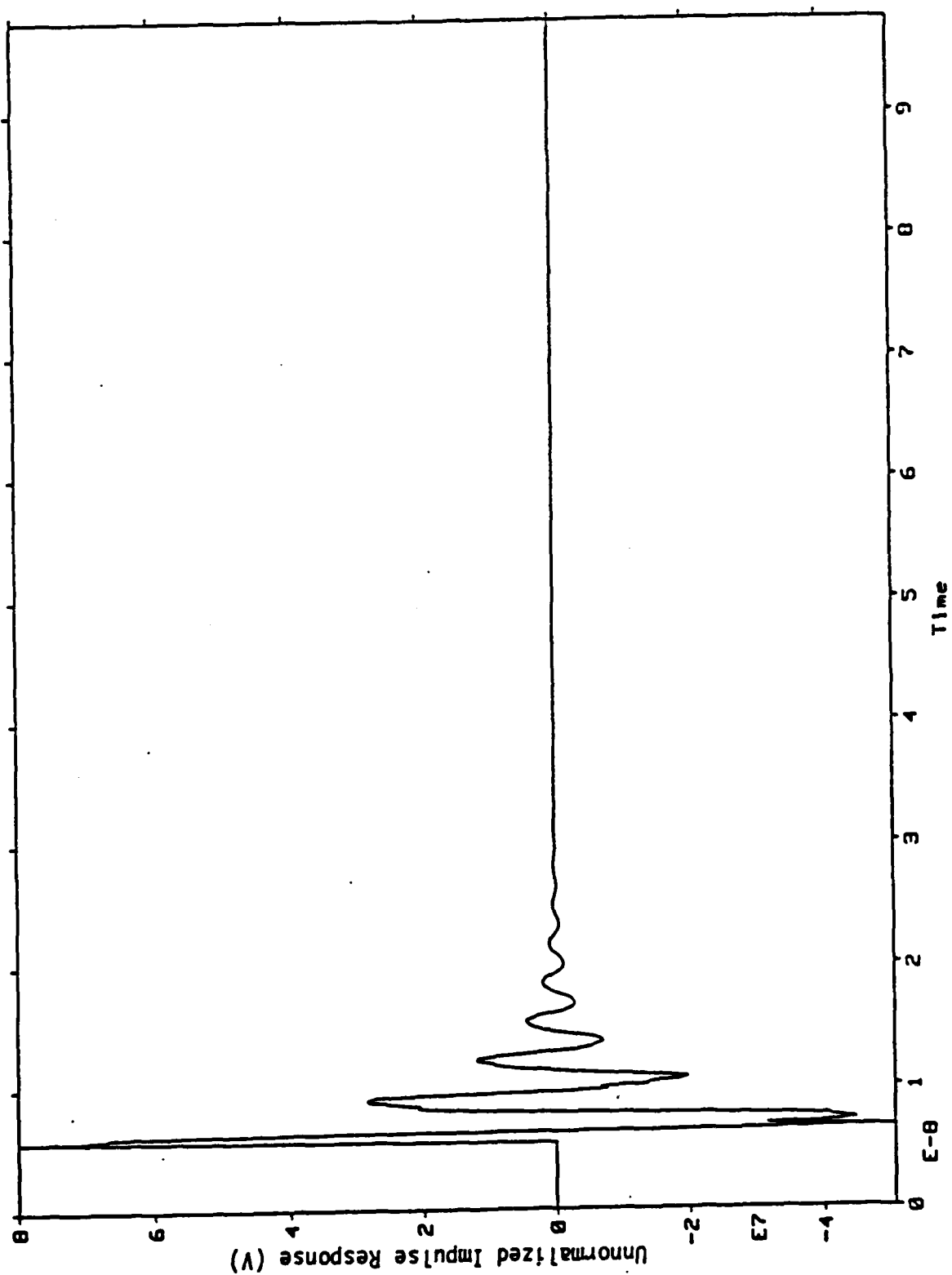


Figure 16. Simulated Monopole Response (15 k-values)

sig

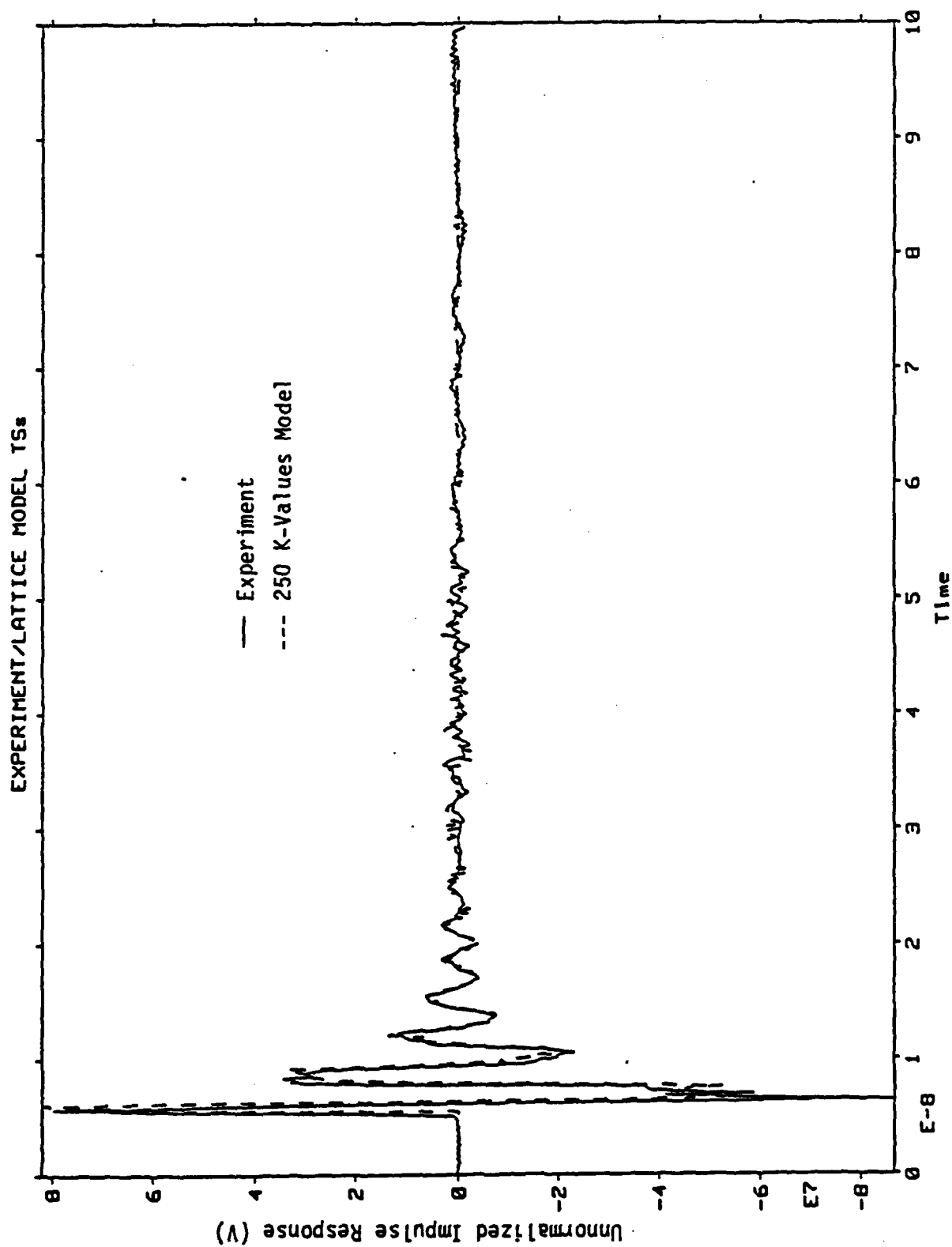


Figure 17. Comparison of Monopole Response Data

sig



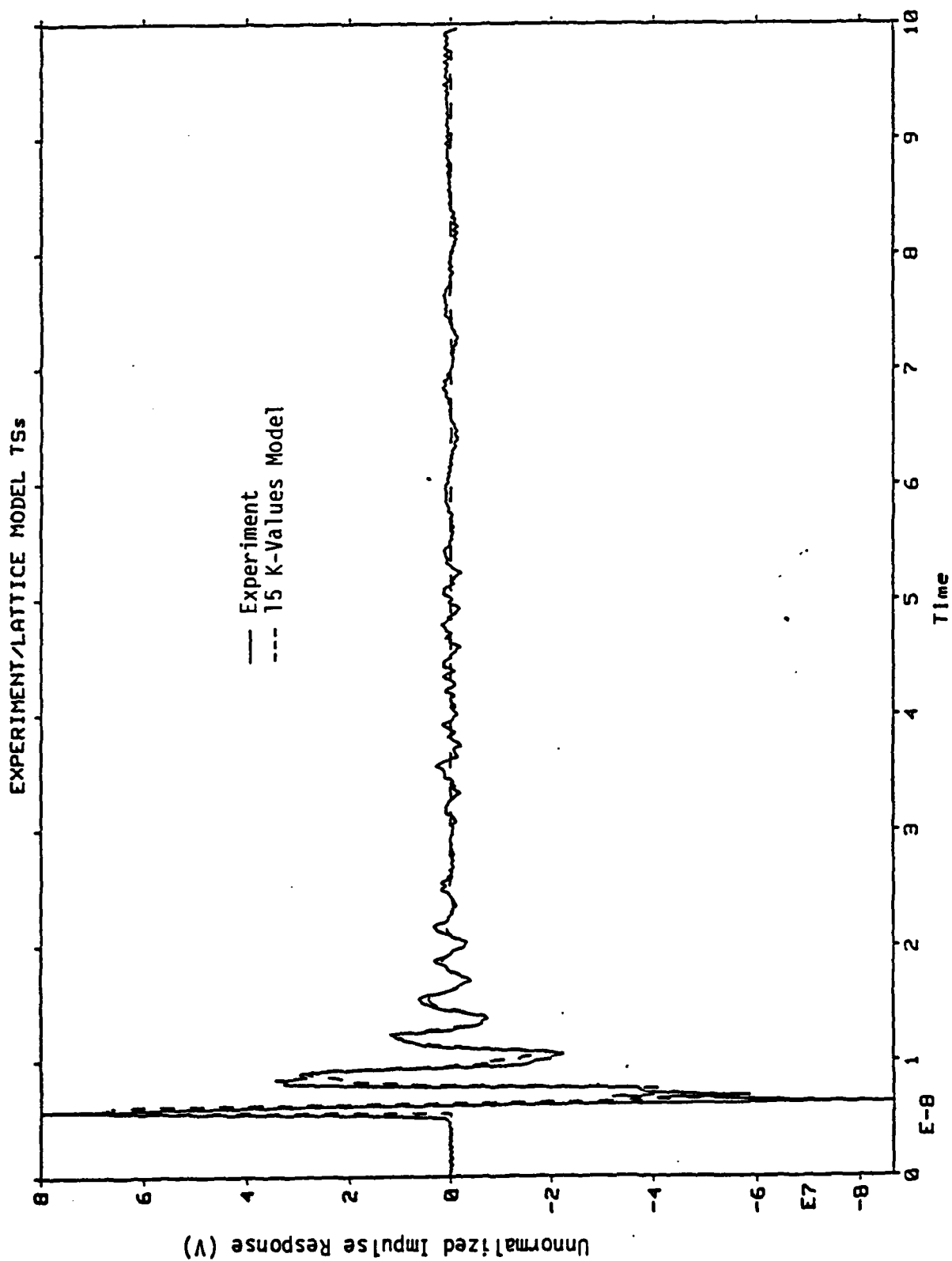


Figure 18. Comparison of Monopole Response Data

sig

0-JHIV-01 13:

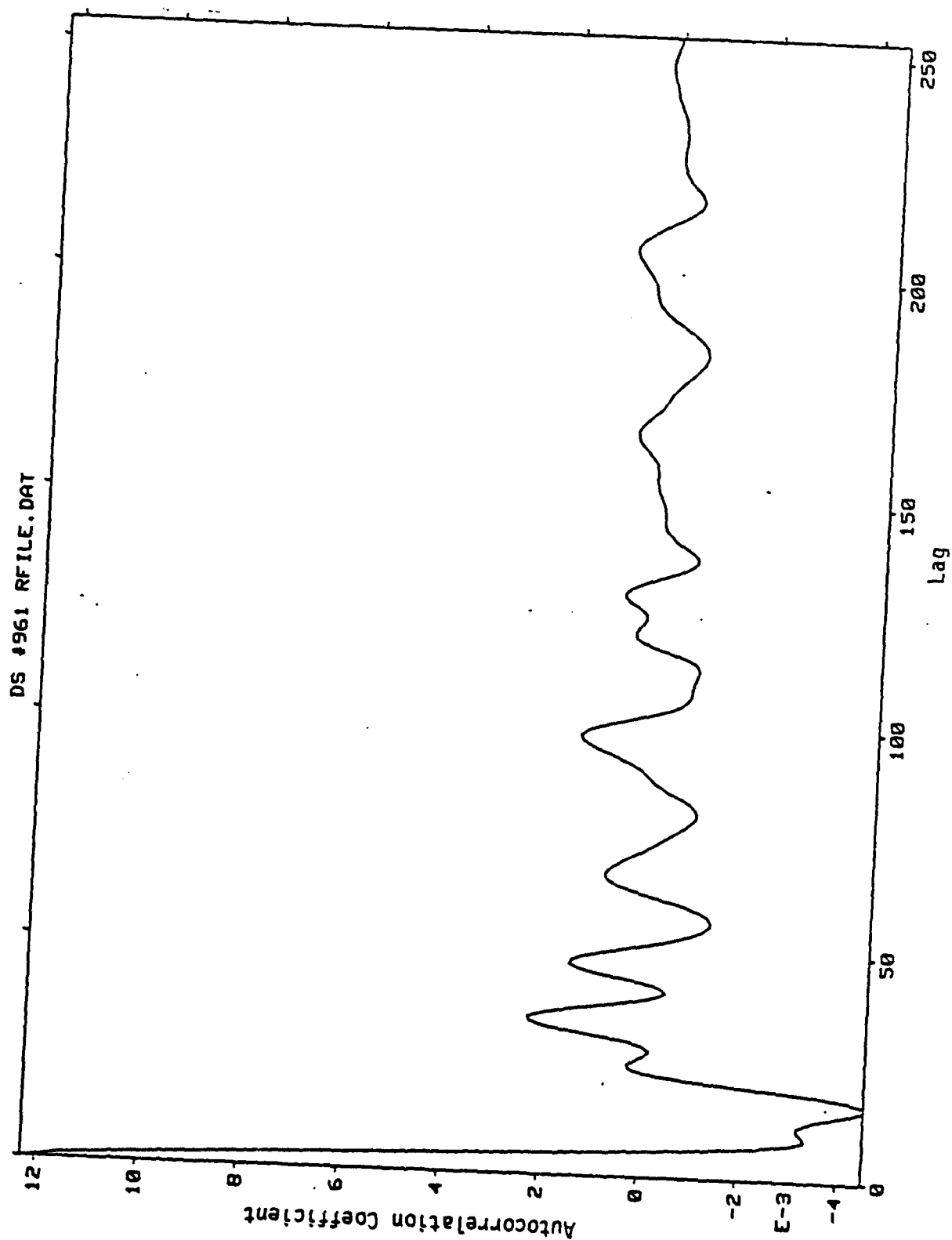


Figure 19. Autocorrelation CB Spiral

D-JH11-01 13:4

DS #960 KFILE.DAT

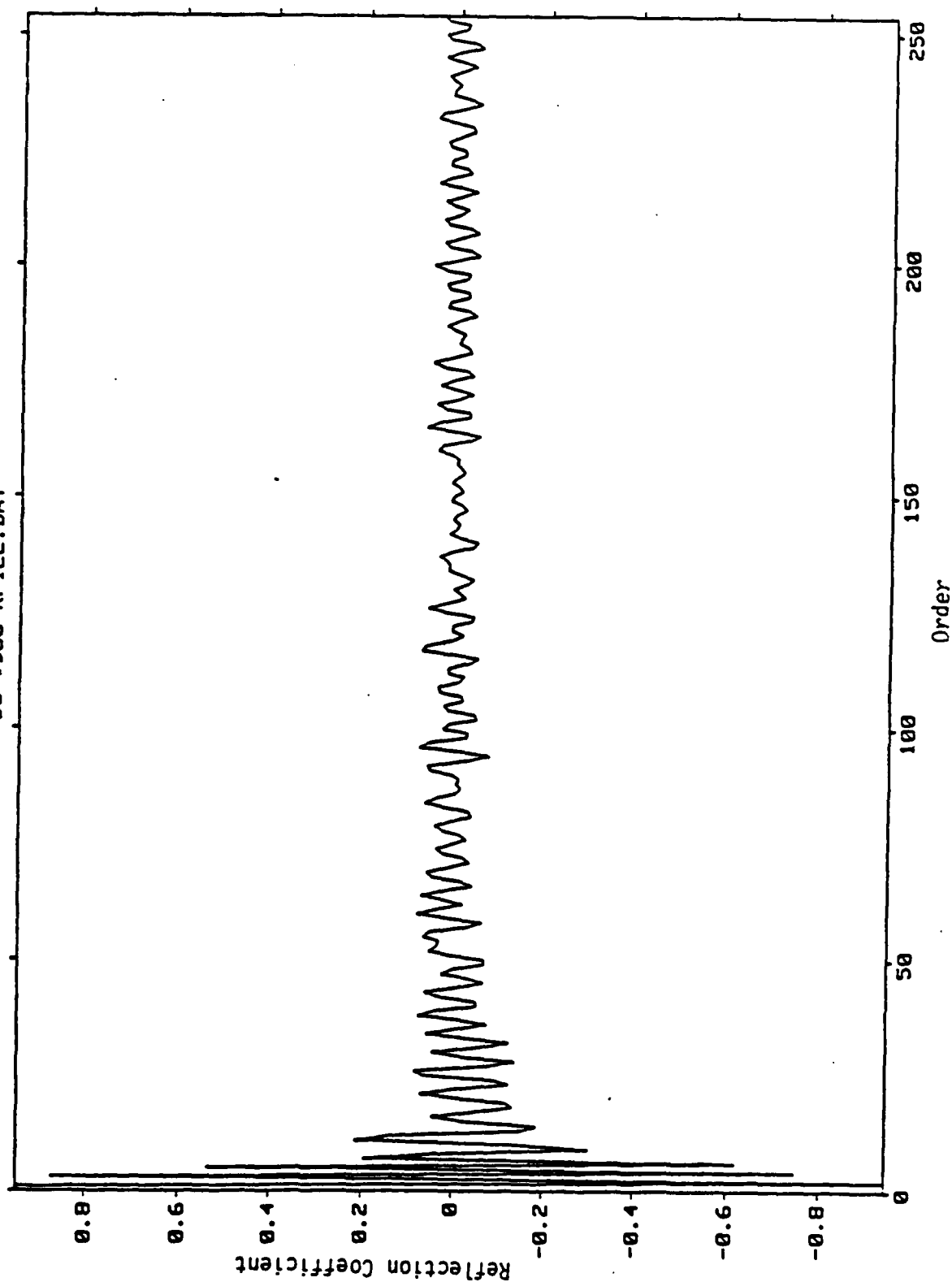


Figure 20. Reflection Coefficient CB Spiral  
(250 k-values)

# CB EXPERIMENT/LATTICE MODEL

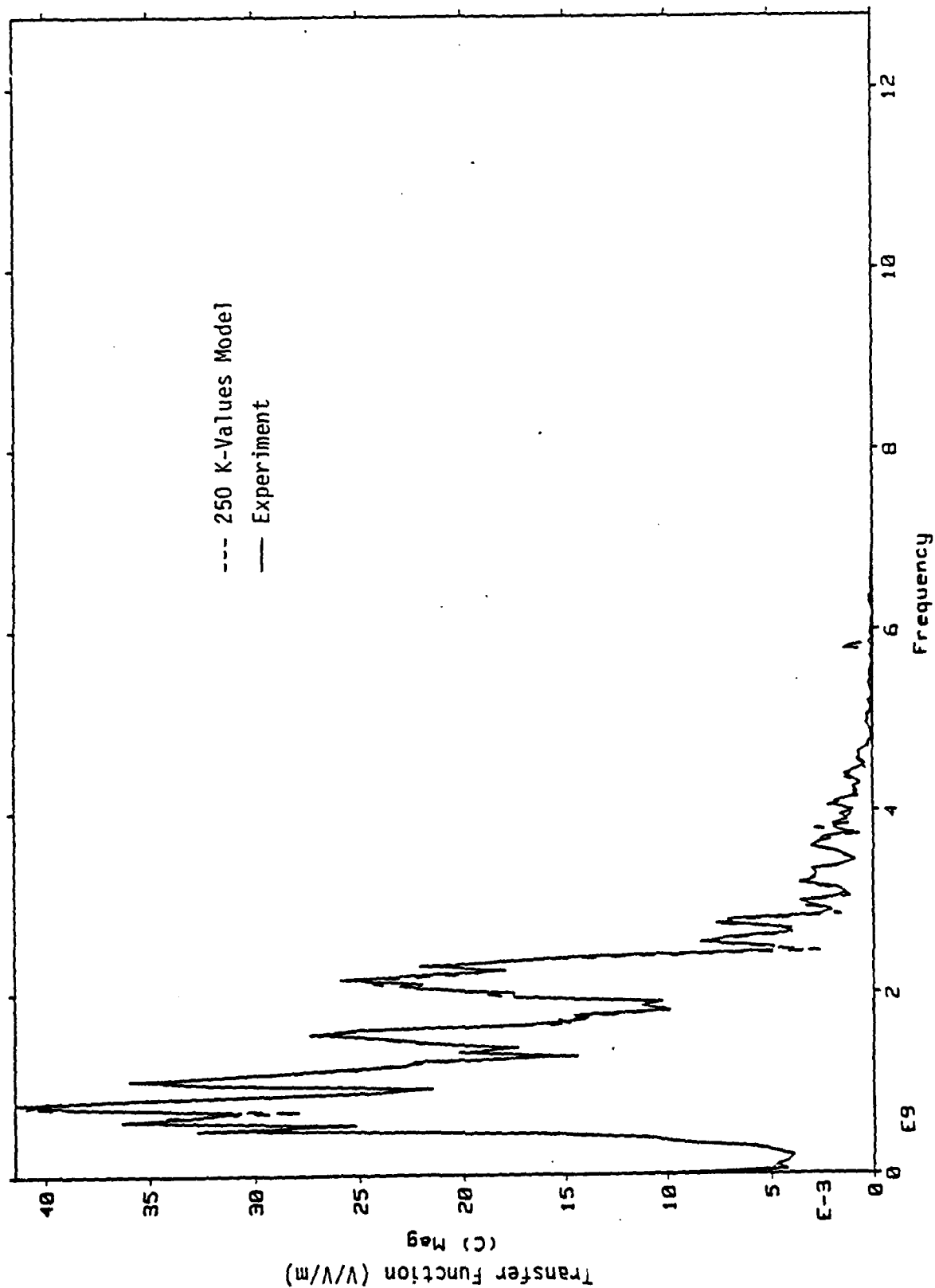


Figure 21. Comparison of FFTs of CB Spiral

END

10-87

DTIC